Signature of chaotic diffusion in band spectra

T. Dittrich, B. Mehlig, and H. Schanz
Max-Planck-Institut für Physik komplexer Systeme, Nöthnitzer Strasse 38, D-01187 Dresden, Germany

U. Smilansky
Department of Physics of Complex Systems, Weizmann Institute of Science, Rehovot 76100, Israel
(Received 29 May 1997; revised manuscript received 1 October 1997)

We investigate the two-point correlations in the band spectra of periodic systems that exhibit chaotic diffusion in the classical limit, in terms of form factors with the winding number as a spatial argument. For times below the Heisenberg time, they contain the full space-time dependence of the classical propagator. They approach constant asymptotes via a regime, reflecting quantal ballistic motion, where they decay by a factor proportional to the number of unit cells. We derive a universal scaling function for the long-time behavior. In the limit of long chains, our results are consistent with expressions obtained by field-theoretical methods. They are substantiated by numerical studies of the kicked rotor and a billiard chain. [S1063-651X(98)03601-0]

PACS number(s): 05.45.+b, 03.65.Sq, 73.20.Dx

I. INTRODUCTION

A large class of systems, among them most prominently solid-state systems, are organized as repetitions of identical or near-identical units. If in such a system the *classical* dynamics is chaotic and the unit cells are connected, then globally this leads to a diffusive spreading of trajectories, irrespective of the presence or absence of static disorder. Regular motion on tori does not contribute to diffusive spreading: Closed tori do not allow for transport along the lattice, while open tori give rise to ballistic spreading. The spectral and transport properties of extended *quantum* systems, in contrast, depend sensitively on the degree of translational symmetry. On short time scales, however, where the quantum dynamics still closely follows the classical, both periodic and disordered quantum systems exhibit (apart from an initial ballistic phase that is of no interest for the following) a spreading of wave packets with the characteristics of the chaotic diffusion in their classical counterparts. The signature of this phase in the discrete spectra of disordered systems with Anderson-localized eigenstates has been investigated previously [1,2], using techniques in the spirit of Berry's semiclassical derivation [3,4] of the spectral form factors for the canonical random-matrix ensembles.

In the present work, we report on a study of periodic systems with band spectra and eigenstates of Bloch form, focusing on the signature of spatial order and dynamical disorder in the spectral two-point correlations. We exploit the existence of a second conserved quantum number in addition to the energy, the quasimomentum, to define form factors in the canonically conjugate space spanned by time and winding number. They are related to the spatially coarse-grained propagator and therefore ideally suited to extract dynamical information from the band structure, without recurring to a local spectrum. Here we evaluate this relation over the entire time evolution of the form factors. In the semiclassical regime, we show that the full space and time dependence of the classical propagator is contained in the form factors. Chaotic diffusion in spatially periodic quantum systems can thus directly be identified in the band structure. Similarly, the spectral signature of the crossover to quantum ballistic motion can be analyzed on basis of the full quantum propagator. In the limit of a large number of unit cells, the form factors exhibit a marked peak in the vicinity of the Heisenberg time, a consequence of the clustering of levels in quasicontinuous bands. We obtain a universal scaling function for the long-time behavior.

Form factors containing the correlations of levels across the Brillouin zone previously have been studied using the supermatrix nonlinear σ model [5,6]. Our approach is complementary in that it emphasizes the important concept of winding numbers, providing direct access to spatial information. In combination with semiclassical techniques, this allows us to draw a particularly transparent picture of the physics over all time regimes. We shall demonstrate that in the case of diffusive spreading and in the limit of an infinite number of unit cells, our theory allows us to reproduce the principal results of the σ-model approach. At the same time, however, we are able to go beyond those results in that we need not make any assumptions as to the number of unit cells in the system nor on the mode of density relaxation.

Our theory therefore applies to a broad class of systems. They include semiconductor superlattices supporting chaotic electron motion (''antidot arrays'') [7–10], quantum-optical systems involving periodically modulated standing-wave fields [11], and Kolmogorov-Arnold-Moser systems with toroidal chaotic layers in phase space containing chains of regular resonance islands, as they occur frequently in molecules [12]. For this type of system, there exists a large body of spectral data, both experimental and numerical [7–12]. By analyzing these data as explained in the following, the dynamical information encoded in the respective band structures can be extracted.

II. GENERALIZED FORM FACTOR

The setup we have in mind is a finite chain of N identical unit cells, with cyclic boundary conditions at its ends. Spatial

disorder within the unit cell is *not* required. We restrict ourselves to quasi-one-dimensional lattices since the generalization to higher dimensions is straightforward.

As a consequence of periodicity, the spectrum can be decomposed into N subsets, each of which corresponds to one of the N irreducible representations of the group of lattice translations $\hat{T}(na\mathbf{e}_x)$, with n an integer. Together these subspectra coalesce into discretized bands and approach continuous bands in the limit $N\to\infty$. Dynamical and spectral quantities specific to one of the irreducible representations [13,14] are constructed using the projectors

$$\hat{P}_m=\frac{1}{N}\sum_{n=0}^{N-1}\chi_m(n)\hat{T}^{\dagger}(na\mathbf{e}_x) \tag{1}$$

onto the corresponding subspaces. They invoke the group characters $\chi_m(n)=\exp(in\theta_m)$. We refer to the $\theta_m=2\pi m/N$, $m=0,\ldots,N-1$, as Bloch phases. The symmetry-projected Green's function is defined as

$$\hat{G}_m(E)=\hat{P}_m\hat{G}(E), \tag{2}$$

where $\hat{G}(E)$ is the Green's function for the full chain. From $\hat{G}_m(E)$, other Bloch-phase-specific quantities can be derived as if they pertained to the full spectrum of a system without spatial symmetry. For example, the Bloch-phase-specific spectral density is related to the trace of the corresponding Green's function (2) in the usual way (see, e.g., Ref. [15]),

$$d_m(E)=\sum_{\alpha}\delta(E-E_{\alpha}(\theta_m))=-\frac{1}{\pi}\,\mathrm{Im\ tr}[\hat{G}_m(E)]. \tag{3}$$

Here the trace extends only over a single unit cell.

The basic energy scale in the following is the inverse mean spectral density *per unit cell* $1/\langle d_{\mathrm{uc}}\rangle$ or, equivalently, the mean separation of neighboring bands. We define also the Heisenberg time with respect to the unit cell $t_{\mathrm{H}}=2\pi\hbar\langle d_{\mathrm{uc}}\rangle$. Accordingly, we scale time as $\tau=t/t_{\mathrm{H}}$ and energy as $r=\langle d_{\mathrm{uc}}\rangle E$. In these units, the size of the spectral window considered is Δr, roughly the total number of bands.

The time-domain counterpart of $d_m(E)$ is the amplitude

$$a_m(\tau)=\int_{-\infty}^{\infty}dr\ e^{-2\pi ir\tau}d_m(r/\langle d_{\mathrm{uc}}\rangle). \tag{4}$$

By performing another, now discrete, Fourier transform with respect to θ_m [14,17], which amounts to going from the Bloch phase to the winding-number representation, we define the amplitude

$$\begin{aligned}\tilde{a}_n(\tau)&=\frac{1}{N}\sum_{m=0}^{N-1}\exp(in\theta_m)a_m(\tau)\\&=\int_{\mathrm{uc}}dq\langle\mathbf{q}+na\mathbf{e}_x|\hat{U}(\tau t_{\mathrm{H}})|\mathbf{q}\rangle,\end{aligned} \tag{5}$$

where $a\mathbf{e}_x$ generates the lattice, with $|\mathbf{e}_x|=1$. Winding-number-specific form factors are defined as

$$\tilde{K}_n(\tau)=\frac{1}{\Delta r}|\tilde{a}_n(\tau)|^2. \tag{6}$$

Substituting Eq. (5) shows that the $\tilde{K}_n(\tau)$ comprise pairs of levels with all Bloch phases. In particular, $\tilde{K}_0(\tau)$ corresponds to the form factor for the entire spectrum, irrespective of spatial periodicity. Equation (5) represents a partial trace of the propagator $\hat{U}$. The $\tilde{K}_n(\tau)$ can therefore be interpreted as probabilities to return after encircling the unit cell n times.

III. SEMICLASSICAL REGIME

A semiclassical account of the symmetry-projected spectral quantities is achieved on the basis of a generalized concept of periodic orbits [13,16,17]. It becomes transparent in a symmetry-reduced representation of the chain, where the two boundaries of the unit cell connected by the translational symmetry are identified. In this way, the unit cell assumes the topology of an annulus, possibly times additional dimensions. An orbit periodic in this reduced space can be classified according to its topology, expressed by its winding number, the number of times it runs around the unit cell before closing. The contribution of a periodic orbit j to $d_m(E)$ contains the additional phase $-n_j\theta_m$, where n_j is the winding number of this orbit [13,16,17]. By the two Fourier transforms that lead from $d_m(E)$ to $\tilde{a}_n(\tau)$, we obtain the semiclassical trace formula

$$\begin{aligned}\tilde{a}_n(\tau)=\sum_j\ &\frac{\tau_j^{(\mathrm{p})}}{\sqrt{|\det(\mathsf{M}_j-\mathsf{I})|}}\exp\left(i\,\frac{S_j(E)}{\hbar}+i\mu_j\frac{\pi}{2}\right)\\&\times\delta_{1/\Delta r}(\tau-\tau_j)\,\delta_{(n-n_j)\bmod N},\end{aligned} \tag{7}$$

with $\tau_j^{(\mathrm{p})}$, M_j, S_j, and μ_j denoting, respectively, the primitive period, monodromy matrix, action, and Maslov index of the periodic orbit j. In addition to the usual amplitude and phase factors, this trace formula has attained two δ functions: A broadened $\delta_{1/\Delta r}(\tau-\tau_j)$ of width $1/\Delta r$ picks out orbits with scaled period $\tau_j\approx\tau$ and an N-periodic Kronecker delta $\delta_{(n-n_j)\bmod N}$ selects periodic orbits with a winding number that differs from n at most by an integer multiple of N.

According to the above interpretation, the $\tilde{K}_n(\tau)$, for $\tau<1$, should be related to the classical probabilities $P_n^{(\mathrm{cl})}(t)$ to return, after n windings, in the symmetry-reduced phase space. Indeed, within the diagonal approximation [1,2,18], we derive

$$\tilde{K}_n^{(\mathrm{sc})}(\tau)=\gamma_n\tau P_n^{(\mathrm{cl})}(\tau t_H),\quad \tau<1. \tag{8}$$

Here we have neglected the contribution of repetitions of shorter periodic orbits. We have not taken the occurrence of self-retracing orbits into account in order to replace individual degeneracy factors, expressing time-reversal (T) invariance, by a global γ_n. Reflecting weak localization as a function of n, it takes the value 2 if orbits with $n_j=n$ are generically T degenerate and 1 otherwise. The winding-number representation thus enables a direct and natural access to weak-localization enhancements in the form factor. In

the Bloch-phase representation, by contrast, weak localization is reflected in a smooth transition from Gaussian-orthogonal-ensemble (GOE) statistics near the symmetry points of the Brillouin zone to Gaussian-unitary-ensemble statistics elsewhere [5,8,9,18].

In order that an orbit contribute to $P_n^{(\mathrm{cl})}(t)$, it must be periodic up to a lattice translation by $na\mathbf{e}_x$. Assuming that the long periodic orbits spread as the generic, nonperiodic ones, we express $P_n^{(\mathrm{cl})}(t)$ in terms of the full classical propagator $p(\mathbf{r}',\mathbf{r};t)$ as a partial trace,

$$P_n^{(\mathrm{cl})}(t)=\int_{\mathrm{uc}} dr\; p(\mathbf{r}+na(\mathbf{0},\mathbf{e}_x),\mathbf{r};t), \tag{9}$$

where $\mathbf{r}=(\mathbf{p},\mathbf{q})$ denotes a point within the unit cell on the energy shell [3]. Equations (8) and (9) show that the generalized form factors, in the semiclassical regime, relate the band structure to the full, if coarse-grained, classical propagator.

The validity of Eq. (8) is not restricted to any specific form of relaxation of the classical distribution, provided the underlying classical dynamics is predominantly chaotic. For example, billiard chains connected only by narrow bottlenecks show a marked deviation from normal diffusion on the time scale of the escape from a single cell. The generalization to higher-dimensional lattices is straightforward. Also there, $P_n^{(\mathrm{cl})}(t)$ takes forms significantly different from diffusion in one dimension.

As a specific example, we evaluate Eq. (8) for normal diffusion in one extended dimension. For an interval of length $L=Na$ with cyclic boundary conditions, the diffusion equation is solved by the propagator $p(x',x;t)=\mathcal{G}^{(\mathrm{mod}\,L)}(x'-x,Dt)$, where $\mathcal{G}^{(\mathrm{mod}\,p)}(x,\sigma^2)$ denotes a normalized Gaussian of period p and variance σ^2. We assume that in the nonperiodic dimensions of phase space, the relaxation towards equidistribution is rapid on the relevant time scales. For times $t\ll t_d=L^2/\pi D$, the Thouless time for the full chain of length L, diffusion is free, $p(x',x;t)=(2\pi Dt)^{-1/2}\exp[-(x'-x)^2/2Dt]$, while for $t\gg t_d$, equidistribution $p(x',x;t)=1/L$ is approached. If, as it is the case here, $p(x',x;t)=p(x'-x;t)$, the partial trace of the propagator amounts to multiplication by the cell size. We find for $\tau<1$,

$$\widetilde{K}_n^{(\mathrm{sc})}(\tau)=\frac{\gamma_n\tau}{N}\,\mathcal{G}^{(\mathrm{mod}\,1)}\left(\frac{n}{N},\frac{g_{\mathrm{uc}}\tau}{\pi N^2}\right)=\begin{cases}\gamma_n\sqrt{\tau/2g_{\mathrm{uc}}}\,e^{-\pi n^2/2g_{\mathrm{uc}}\tau}, & \tau\ll N^2/g_{\mathrm{uc}},\\ \gamma_n\tau/N, & \tau\gg N^2/g_{\mathrm{uc}},\end{cases} \tag{10}$$

introducing the dimensionless parameter $g_{\mathrm{uc}}=N^2t_{\mathrm{H}}/t_{\mathrm{d}}=2\pi^2\hbar\langle d_{\mathrm{uc}}\rangle D/a^2$. Since we do not require static disorder and diffusion within the unit cell, the interpretation of g_{uc} as a conductance is purely formal.

With respect to g_{uc} and N, we distinguish two regimes. For $g_{\mathrm{uc}}\gg N^2$, the classical dynamics becomes ergodic before the energy-time uncertainty relation allows us to resolve the interband spacing $1/\langle d_{\mathrm{uc}}\rangle$. The sampling by the discrete Bloch phases is then too coarse to reveal the continuous bands underlying the discrete levels and the full spectrum appears as a superposition of N independent spectra. The condition $g_{\mathrm{uc}}\gg N^2$ can also be expressed as $2\pi/N\gg\theta_{\mathrm{corr}}$, where $2\pi/N$ is the Bloch-phase spacing and $\theta_{\mathrm{corr}}=2\pi\sqrt{\pi/g_{\mathrm{uc}}}$ is the spectral correlation length with respect to variation of the Bloch phase [6]. Only for $g_{\mathrm{uc}}\ll N^2$ does the arrangement of levels in bands affect the two-point correlations. A number of $N\theta_{\mathrm{corr}}/2\pi$ levels then contribute coherently to the spectral correlations on time scales $\tau\leqslant 1$. In this case the second option in Eq. (10), the ergodic regime of the classical dynamics, is irrelevant. In the space-time domain, this amounts to the diffusion cloud still being well localized within the chain at $\tau=1$. Increasing the chain length beyond $N=\sqrt{g_{\mathrm{uc}}}$ merely results in a finer resolution of the bands.

IV. QUANTUM BALLISTIC REGIME

Equation (10) was derived using the diagonal approximation with respect to the classical phases. The periodic orbits occurring in the underlying trace formula are those of the symmetry-reduced space. The break time beyond which the diagonal approximation ceases to be valid is therefore the Heisenberg time for the unit cell t_{H} or, equivalently, $\tau=1$. This means that Eq. (10) describes only the spectral correlations on scales of a typical interband spacing or larger. Therefore, we adopt a different approach to $\widetilde{K}_n(\tau)$ for $\tau>1$, corresponding to energy scales of the interband spacing and below. Starting anew from the definition (5), we use Poisson resummation to replace the sum over m by an integral over θ,

$$\widetilde{a}_n(\tau)=\frac{1}{2\pi}\sum_{\mu=-\infty}^{\infty}\int_0^{2\pi}d\theta\; e^{i(n-\mu N)\theta}\sum_{\alpha}\; e^{-2\pi i r_\alpha(\theta)\tau}, \tag{11}$$

where $r_\alpha(\theta)=\langle d_{\mathrm{uc}}\rangle E_\alpha(\theta)$. For large τ the phase of the integrand is rapidly oscillating and the integration can be performed within an asymptotic approximation. Provided the bandwidth is of the order of the interband spacing, this approach is justified for times $\tau\gtrsim 1$. It will in fact be seen in Sec. V that this approximation exactly reproduces the large-τ behavior in the limit of $N\to\infty$. For simplicity we disregard special cases such as inflection points or higher-order extrema, which can be treated, e.g., by a uniform Bessel-function approximation [19]. Saddle-point integration leads to the condition

$$2\pi r'_\alpha(\theta_j(\nu))=\nu \tag{12}$$

for points $\theta_j(\nu)$ of stationary phase, with $\nu=(n-\mu N)/\tau$. Replacing dimensionless quantities by unscaled ones gives the equivalent condition $v_\alpha(k)=(n-\mu N)a/t$, where $v_\alpha(k)$ is the group velocity for the band α at quasimomentum $k=\hbar\theta/a$. It expresses the ballistic motion of Bloch waves. For $\tau>1$, the phases $2\pi i r_\alpha(\theta_j)\tau$ left by the saddle-point integration can be considered random. Upon squaring to obtain the form factors, we therefore drop the off-diagonal contributions and get

$$\widetilde{K}_n(\tau)=\frac{\gamma_n}{\tau}\sum_{\mu=-\infty}^{\infty}F\left(\frac{n-\mu N}{\tau}\right), \tag{13}$$

where $F(\nu)=(4\pi^2\Delta r)^{-1}\Sigma_\alpha\Sigma_j|r''_\alpha(\theta_j(\nu))|^{-1}$ is a positive function depending on n and τ only through $(n-\mu N)/\tau$. Similar to what we found for $\tau<1$, the $\widetilde{K}_n(\tau)$ can be interpreted as sums of winding-number distributions $F(\nu(n,\tau))$, each of which is stretching from a center at $n=\mu N$, but now as a *linear* function of time, so that the variance σ^2 grows quadratically. They are normalized by the common prefactor $1/\tau$. In order to determine the as yet unknown function $F(\nu)$, we use a heuristic argument in the spirit of Refs. [1,2, 4] and extrapolate both the semiclassical expression (10) and Eq. (13) towards $\tau=1$. Expanding

$$\widetilde{K}_n^{(\mathrm{sc})}(\tau)=\frac{\gamma_n\tau}{N}\,\mathcal{G}^{(\mathrm{mod}\,1)}\left(\frac{n}{N},\frac{g_{\mathrm{uc}}\tau}{\pi N^2}\right)=\gamma_n\sqrt{\frac{\tau}{2g_{\mathrm{uc}}}}\sum_{\mu=-\infty}^{\infty}\exp\left(-\frac{\pi(n-\mu N)^2}{2\tau g_{\mathrm{uc}}}\right),\tag{14}$$

we match Eq. (10) with Eq. (13) at $\tau=1$,

$$\sum_{\mu=-\infty}^{\infty}F(n-\mu N)=\frac{1}{\sqrt{2g_{\mathrm{uc}}}}\sum_{\mu=-\infty}^{\infty}\exp\left(-\frac{\pi(n-\mu N)^2}{2g_{\mathrm{uc}}}\right).\tag{15}$$

Comparing both sums term by term, we obtain $F(\nu)=(2g_{\mathrm{uc}})^{-1/2}\exp(-\pi\nu^2/2g_{\mathrm{uc}})$ and thus, for the regime $\tau>1$,

$$\widetilde{K}_n(\tau)=\frac{\gamma_n}{N}\,\mathcal{G}^{(\mathrm{mod}\,1)}\left(\frac{n}{N},\frac{g_{\mathrm{uc}}\tau^2}{\pi N^2}\right).\tag{16}$$

In the presence of additional symmetries, the spectral statistics can be that of the GOE throughout the Brillouin zone, possibly with weak localization enhancements in the vicinity of the symmetry points (cf. the discussion of the quantum kicked rotor below). In this case, an analogous matching procedure applies.

For the long-time behavior of the entire set of $\widetilde{K}_n(\tau)$, Eq. (16) implies the following scenario. Initially, $\widetilde{K}_0(\tau)$ decays as $1/\tau$ as long as only the term with $\mu=0$ contributes significantly. As terms with larger μ attain a comparable magnitude, all $\widetilde{K}_n(\tau)$ approach an asymptotic constant γ_n/N [an exact evaluation [18] gives a correction $-2/N^2$ in the presence of the band symmetry $d_{-m}(E)=d_m(E)$ if N is even]. The asymptotic domain is reached at $\tau\approx N\sqrt{\pi/g_{\mathrm{uc}}}$. This is the effective Thouless time for ballistic spreading. It corresponds to the time when the uncertainty relation allows the resolution of the typical separation $2\pi/(N\theta_{\mathrm{corr}}\langle d_{\mathrm{uc}}\rangle)$ of neighboring discrete levels. It will be shown in the following that the expression (16) reproduces the numerical data surprisingly well for $\tau>1$.

Figure 1 summarizes our results for the time dependence of the $\widetilde{K}_n(\tau)$. We can identify three distinct time regimes: a semiclassical phase where the form factors reflect the classical diffusive spreading, a regime dominated by quantal ballistic motion, and an asymptotic regime reflecting the discreteness of the spectrum on the finest energy scales. These long-time asymptotes vanish for large N as $1/N$. At the same time, the maximum of $\widetilde{K}_0(\tau)$ near $\tau=1$, all other parameters being kept fixed, is proportional to θ_{corr} and independent of N. Therefore, in the regime $g_{\mathrm{uc}}\ll N^2$ where proper bands exist, there is a crossover during which $\widetilde{K}_0(\tau)$ decays by a factor of the order of $N\theta_{\mathrm{corr}}$. Thus, together with its rise in the initial, semiclassical regime, $\widetilde{K}_0(\tau)$ attains a peak in the vicinity of $\tau=1$ that expresses the *clustering* of levels into bands [7]. The stationary-phase condition (12), with $\mu=0$ (only this term contributes near $\tau=1$), shows that the peak is associated with the extremal points in the bands, that is, with the van Hove singularities [20] in the full spectral density $d(E)$.

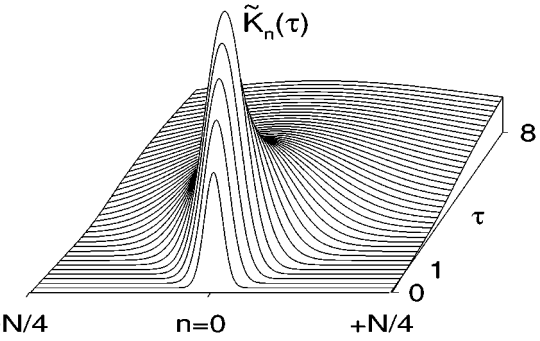

FIG. 1. Space-time dependence of the theoretical prediction for $\widetilde{K}_n(\tau)$ according to Eqs. (10) and (16) for $N=512$.

Finally, we note that for small N, in particular for $N=2$, the coarse-grained density relaxation does not follow a diffusion law if there is no static disorder within the cells. An evaluation of the semiclassical and the quantum domains along similar lines as sketched here gives access to the statistics of tunnel splittings in double billiards.

V. THE LARGE-N LIMIT

In the present section we discuss the limit of $N\to\infty$. In this limit, our results simplify considerably, since only the term $\mu=0$ contributes in Eqs. (13) and (14). For short times $\tau\lesssim 1$ the $\widetilde{K}_n(\tau)$ can be replaced by a single, diffusively spreading Gaussian as given in the second line of Eq. (10). In the long-time regime $\tau\gtrsim 1$, we obtain

$$\widetilde{K}_n(\tau)=\frac{\gamma_n}{\sqrt{2g_{\mathrm{uc}}\tau}}\exp\left(-\frac{\pi}{2g_{\mathrm{uc}}}\left[\frac{n}{\tau}\right]^2\right).\tag{17}$$

This implies in particular that $\widetilde{K}_0(\tau)=1/\sqrt{2g_{\mathrm{uc}}\tau}$.

The same limiting behavior has been calculated within the framework of a nonlinear σ model [5]. We shall now compare Eq. (17) with the corresponding results in Ref. [5]. We make use of the fact that the Bloch phase θ can be viewed as a generalized Aharonov-Bohm flux and in the present limit becomes a continuous variable. Accordingly, we replace $d_m(r)$ by $d(r,\theta)$. For simplicity, we restrict ourselves to the case of broken time-reversal invariance throughout the Brillouin zone. This corresponds to $\gamma_n=1$ for all n. In order to enable a full quantitative comparison with Ref. [5], we had to calibrate the dimensionless conductance on basis of a common definition: In the present limit and for $\tau\gg 1$, we find

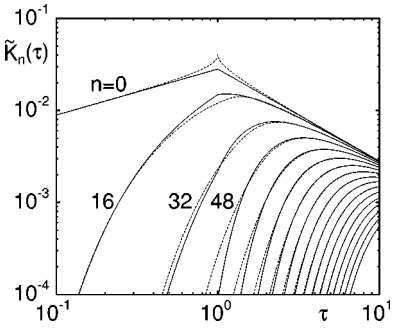

FIG. 2. Comparison of the form factors $\widetilde{K}_n(\tau)$ in the limit $N\to\infty$, according to Eqs. (10) and (17) (solid lines), to the corresponding functions as implied by the results of Ref. [5]; cf. Eq. (19) (dashed lines). The graphs shown are for (from top to bottom) $n=0,16,32,...,256$. The dimensionless conductance is $g_{\rm uc}=200\pi$, the same value as that underlying the data in Fig. 4(a).

the following relation between the variance of the level velocities, the second moment of the $\widetilde{K}_n(\tau)$ with respect to n, and the conductance:

$$4\pi^2\left\langle\left(\frac{dr_\alpha(\theta)}{d\theta}\right)^2\right\rangle_{\alpha,\theta}=\sum_{n=-\infty}^{\infty}\frac{n^2}{\tau^2}\,\widetilde{K}_n(\tau)=\frac{g_{\rm uc}}{\pi}. \quad (18)$$

In Ref. [5], the following expression is obtained for the flux-averaged correlation function:

$$\langle d(\overline{r,\theta})d(\overline{r}+r,\overline{\theta}+\theta)\rangle_{\overline{r,\theta}}-1 = \frac{2\pi}{g_{\rm uc}\theta^2}\int_0^\infty\frac{d\lambda}{\lambda}\left\{\exp\left(-\frac{g_{\rm uc}}{\pi}\left[\frac{\theta}{2\pi}\right]^2\left|\pi\lambda-\frac{\lambda^2}{2}\right|\right)-\exp\left(-\frac{g_{\rm uc}}{\pi}\left[\frac{\theta}{2\pi}\right]^2\left|\pi\lambda+\frac{\lambda^2}{2}\right|\right)\right\}\cos(r\lambda). \quad (19)$$

An expression for $\widetilde{K}_n(\tau)$ is reached by a Fourier transformation with respect to r and with respect to θ over the Brillouin zone. The discrete spatial Fourier transform cannot be applied directly to Eq. (19) since this expression violates periodicity in θ. Instead, exploiting the fact that this expression decays to zero for $\theta\to\infty$, we approximate the Fourier sum over the Brillouin zone by a continuous Fourier transformation over the whole real axis. We obtain

$$\widetilde{K}_n(\tau)=\frac{1}{2g_{\rm uc}\tau}\{\Phi_n(x_+)-\Phi_n(x_-)\}, \quad (20)$$

with $\Phi_n(x)=\pi n\ \mathrm{erf}(n/2\sqrt{x})+2\sqrt{\pi x}\,\exp(-n^2/4x)$ and $x_\pm=(2\pi)^{-1}g_{\rm uc}|\tau\pm\tau^2|$.

We have checked analytically and numerically (Fig. 2) that for both $\tau\to0$ and $\tau\to\infty$, Eq. (20) coincides asymptotically with our results. Only in the vicinity of $\tau=1$ do deviations exist [e.g., from Eq. (17) we find $\widetilde{K}_0(1)=1/\sqrt{2g_{\rm uc}}$, while Eq. (20) gives $\widetilde{K}_0(1)=1/\sqrt{g_{\rm uc}}$; cf. Fig. 2]. The close agreement between the respective results provides further support for the matching procedure we used to connect the short- and long-time regimes. This agreement is not surprising since recently it has been shown [21–23] that the random-matrix approach underlying Eq. (19) also applies to systems where the disorder is of dynamical origin.

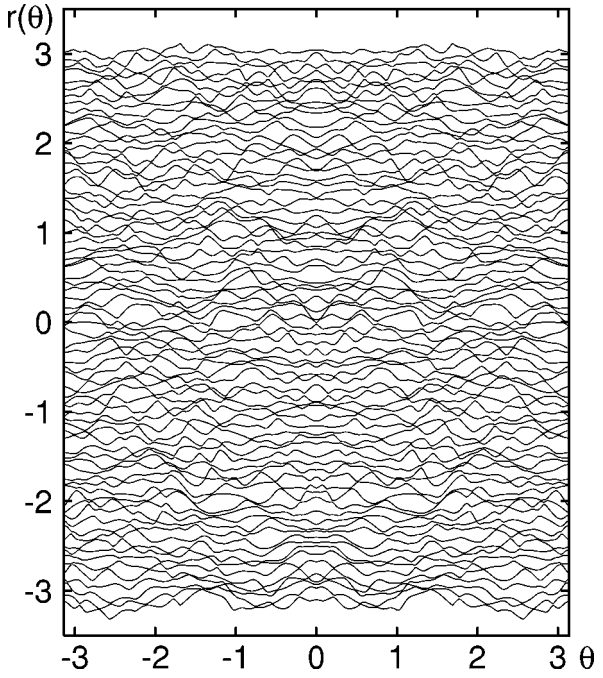

FIG. 3. Quasienergy bands pertaining to chaotic Bloch states of the quantum kicked rotor, for $k=300$ and $\tau=4\pi/75$, corresponding to a periodic potential with a unit cell that accommodates 75 Bloch states.

VI. NUMERICAL RESULTS AND DISCUSSION

In the remainder, we compare the theory sketched in the previous sections to two prototypical yet quite different models. Our first example is the kicked rotor on a torus [24], defined by its Hamiltonian

$$H(l,\vartheta;t)=\frac{(l-\lambda)^2}{2}+V_{\alpha,k}(\vartheta)\sum_{m=-\infty}^{\infty}\delta(t-m\tau). \quad (21)$$

It is periodically time dependent, so the spectrum and eigenstates are adequately discussed in terms of quasienergies and Floquet states, respectively. The kicked rotor attains periodicity also in the angular-momentum variable l if the parameter τ, an effective quantum of action, is chosen as $\tau=4\pi p/q$, with p,q coprime (here we restrict them further to $p=1$ and q odd). The unit cell then accommodates q quanta of angular momentum. The number of quasienergy bands (for a typical sample, see Fig. 3) is also q. It is analogous to the total number of bands Δr introduced above.

The quasienergies are obtained by diagonalizing the symmetry-projected Floquet operator at Bloch phase θ_m [24],

$$\langle l'|\hat{U}_m|l\rangle = \exp\left(-2\pi i\,\frac{p}{q}(l-\lambda)^2\right) \times \frac{1}{q}\sum_{n=0}^{q-1} e^{-iV_{\alpha,k}([\theta_m+2\pi n]/q)} e^{i(l-l')(\theta_m+2\pi n)/q}. \tag{22}$$

For the kicked rotor on a torus, the number of unit cells is simply determined by the number N of Bloch phases where Eq. (22) is evaluated. This additional parameter is independent of q, the number of bands. The total number of levels in the spectrum is therefore Nq.

In addition to being periodic in l and l', the Floquet matrix (22) allows for several twofold symmetries [24–26]. In order to break them in a controlled manner without significantly altering the classical diffusion, an angular-momentum shift by λ has been introduced and the potential has been chosen as [25]

$$V_{\alpha,k}(\vartheta) = k\left[\cos\left(\alpha\frac{\pi}{2}\right)\cos\,\vartheta + \frac{1}{2}\sin\left(\alpha\frac{\pi}{2}\right)\sin 2\vartheta\right]. \tag{23}$$

For $\alpha=\lambda=m=0$, which classically corresponds to the common standard map, the kicked rotor possesses two independent twofold symmetries: a unitary one, the parity P, in which $l\to -l$, $\vartheta\to 2\pi-\vartheta$, and $t\to t$; and an antiunitary one, time reversal T, in which $l\to -l$, $\vartheta\to\vartheta$, and $t\to -t$. P invariance is broken for $m\neq 0\,L/2$, i.e., off the band center and edges. Therefore, for $\alpha=\lambda=0$, the quasienergy statistics corresponds to the superposition of two independent circular orthogonal ensembles (COE's) at $m=0,\pm L/2$ and to a single COE elsewhere. Choosing $\alpha\neq 0$ breaks P also at the symmetry points and at the same time lifts the band symmetry so that COE statistics becomes valid throughout the Brillouin zone. If λ takes a noninteger value, T invariance, which amounts to $\langle -l'|\hat{U}_m|-l\rangle = \langle l'|\hat{U}_m|l\rangle$, is broken. In this case, the quasienergy statistics is that of the circular unitary ensemble (CUE) everywhere or that of two superposed CUE's at the symmetry points if $\alpha=0$.

Sufficiently large spectral data sets have been generated by varying k over small intervals so that the classical diffusion constant $D\approx k^2/2$ is not changed appreciably. The parameters N, q, and k were chosen such that the scale of localization due to disorder within the unit cell [6,24] by far exceeds the cell size. In Fig. 4(a) we show, for both twofold symmetries simultaneously broken ($\alpha=0.2$, $\lambda=0.5$), the set of $\widetilde{K}_n(\tau)$ as a function of τ at selected equidistant values of n and compare with our theory [Eqs. (10) and (16)]. The three time regimes and the corresponding power-law time dependences of $\widetilde{K}_0(\tau)$ can clearly be distinguished. Comparing with the nonlinear-σ-model results [5] [Eq. (20) and the dashed lines in Fig. 2], we find that near $\tau=1$, they reproduce the data even better, including an unexpected feature such as the sharp peak at $n=0$, $\tau=1$. The saturation regime $\tau\gtrsim N\sqrt{\pi/g_{\rm uc}}$, however, is not contained in Eq. (20).

Our second example is a billiard chain composed of unit cells as shown in the inset in Fig. 4(b). The wave functions

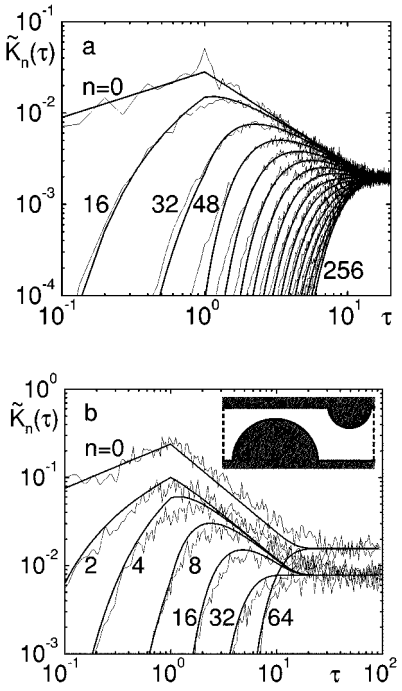

FIG. 4. (a) Form factors $\widetilde{K}_n(\tau)$ for the kicked rotor on a torus at (from top to bottom) $n=0,16,32,\ldots,256$ ($N=512$), compared to the theory (heavy lines). The parameters determining $g_{\rm uc}$ are, in the notation of Ref. [1], $\tau=4\pi/225$ (dimensionless quantum of action, not to be confounded with the scaled time used in this paper) and $k=300$, giving $g_{\rm uc}=200\pi$. All twofold antiunitary symmetries are broken. (b) is analogous to (a), but for a billiard chain composed of $N=128$ unit cells (inset). The winding numbers shown are $n=0$, 2, 4, 8, 16, 32, and 64. The only free parameter of the theory $g_{\rm uc}$ was determined by an independent classical simulation [18].

satisfy the Helmholtz equation augmented with Dirichlet boundary conditions on the channel walls and periodic boundary conditions along the channel after N unit cells. Provided that trajectories traversing the unit cell without hitting the obstacles are excluded by an appropriate geometry, the classical dynamics is diffusive on scales larger than the size of the unit cell. The energy bands can be found using the scattering approach to billiard quantization; see Ref. [18] for details of the method. The shape of the unit cell is chosen such that there are no other unitary symmetries besides the discrete translation invariance. However, due to time-reversal invariance, the bands are symmetric with respect to $\theta=0$ and π such that $\gamma_0=\gamma_{N/2}=2$ and otherwise $\gamma_n=1$. Figure 4(b), which is analogous to Fig. 4(a), clearly shows the corresponding enhancements of $\widetilde{K}_0(\tau)$ and $\widetilde{K}_{N/2}(\tau)$ throughout the three regimes. Correspondingly, the spectral statistics for fixed Bloch number follows the COE at the center and the edge of the Brillouin zone and approaches the CUE in between [18].

Our theoretical results reproduce remarkably well the numerical data obtained for the two models. This lends support to the approximations underlying the theory and corroborates its conclusions. The large-N limit is of particular interest because it provides a very sensitive tool for studying the transition to Anderson localization when the periodicity is disrupted by disorder. In the latter case, the level statistics

approaches the Poissonian limit and the corresponding spectral form factor approaches the constant value 1 in the long-time limit. This is in a marked difference from the periodic case, where $\widetilde{K}_0(\tau) \approx 1/\tau$ for $\tau > 1/N$. The transition between these two rather distinct asymptotics occurs as a smooth function of the degree of disorder. In order to understand this transition in semiclassical terms [1,2], one may discuss the effect of weak disorder through the small random differences between the phases assigned to periodic orbits that were related by symmetry in the absence of disorder. This approach is similar to the semiclassical discussion of the response of the weak-localization peak to a weak magnetic field [25]. A detailed analysis of this scenario will be left for further study.

ACKNOWLEDGMENTS

The research reported in this work was supported by grants from the Minerva Center for Nonlinear Physics. T.D., B.M., and H.S. would like to thank the Weizmann Institute of Science, Rehovot, and U.S. would like to thank the Max Planck Institute for Physics of Complex Systems, Dresden, for the kind hospitality enjoyed during several visits.

[1] T. Dittrich and U. Smilansky, Nonlinearity **4**, 85 (1991); T. Dittrich, E. Doron, and U. Smilansky, J. Phys. A **27**, 79 (1994); T. Dittrich, Phys. Rep. **271**, 267 (1996).

[2] N. Argaman, Y. Imry, and U. Smilansky, Phys. Rev. B **47**, 4440 (1993).

[3] J. H. Hannay and A. M. Ozorio de Almeida, J. Phys. A **17**, 3429 (1984).

[4] M. V. Berry, Proc. R. Soc. London, Ser. A **400**, 229 (1985).

[5] B. D. Simons and B. L. Altshuler, Phys. Rev. Lett. **70**, 4063 (1993).

[6] N. Taniguchi and B. L. Altshuler, Phys. Rev. Lett. **71**, 4031 (1993).

[7] T. Geisel, R. Ketzmerick, and G. Petschel, Phys. Rev. Lett. **66**, 1651 (1991); **67**, 3635 (1991); R. Ketzmerick, G. Petschel, and T. Geisel, *ibid.* **69**, 695 (1992).

[8] E. R. Mucciolo, R. B. Capaz, B. L. Altshuler, and J. D. Joannopoulos, Phys. Rev. B **50**, 8245 (1994).

[9] H. Silberbauer, P. Rotter, U. Rössler, and M. Suhrke, Europhys. Lett. **31**, 393 (1995).

[10] G. A. Luna-Acosta, K. Na, L. E. Reichl, and A. Krokhin, Phys. Rev. E **53**, 3271 (1996).

[11] A. R. Kolovsky, S. Miyazaki, and R. Graham, Phys. Rev. E **49**, 70 (1994); S. Miyazaki and A. R. Kolovsky, *ibid.* **50**, 910 (1994); A. R. Kolovsky, *ibid.* **56**, 2261 (1997).

[12] H.-J. Korsch, B. Mirbach, and B. Schellhaaβ, J. Phys. A **30**, 1659 (1997).

[13] J. M. Robbins, Phys. Rev. A **40**, 2128 (1989).

[14] S. C. Creagh and N. D. Whelan, Phys. Rev. Lett. **77**, 4975 (1996).

[15] M. C. Gutzwiller, *Chaos in Classical and Quantum Mechanics* (Springer, New York, 1990), Vol. 1.

[16] P. Lebœuf and A. Mouchet, Phys. Rev. Lett. **73**, 1360 (1994).

[17] R. Scharf and B. Sundaram, Phys. Rev. Lett. **76**, 4907 (1996).

[18] T. Dittrich, B. Mehlig, H. Schanz, and U. Smilansky, Chaos Solitons Fractals **8**, 1205 (1997).

[19] J. R. Stine and R. A. Marcus, J. Chem. Phys. **59**, 5145 (1973).

[20] N. W. Ashcroft and N. D. Mermin, *Solid State Physics* (Holt-Saunders, Philadelphia, 1976).

[21] B. A. Muzykantskii and D. E. Khmelnitskii, Pis'ma Zh. Eksp. Teor. Fiz. **62**, 68 (1995) [JETP Lett. **62**, 76 (1995)].

[22] O. Agam, B. L. Altshuler, and A. A. Andreev, Phys. Rev. Lett. **75**, 4389 (1995).

[23] E. B. Bogomolny and J. P. Keating, Phys. Rev. Lett. **77**, 1472 (1996).

[24] F. M. Izrailev, Phys. Rep. **196**, 299 (1990).

[25] R. Blümel and U. Smilansky, Phys. Rev. Lett. **69**, 217 (1992); M. Thaha, R. Blümel, and U. Smilansky, Phys. Rev. E **48**, 1764 (1993).

[26] G. Casati, R. Graham, I. Guarneri, and F. M. Izrailev, Phys. Lett. A **190**, 159 (1994).